

POLARIZATION CLOUDS IN THE MARTIAN ATMOSPHERE: HUBBLE SPACE TELESCOPE OBSERVATIONS. V. Kaydash¹, Yu. Shkuratov¹, M. Kreslavsky^{1,2}, G. Videen³, M. Wolff³, J. Bell⁴, ¹Astron. Institute of Kharkov National Univ. 35 Sumskaya St., Kharkov, 61022, Ukraine. ²Geological Sciences, Brown Univ., Providence, RI, USA. ³Space Sci. Institute 3100 Marine St., Suite A353, Boulder, CO 80303-1058, USA. ⁴Cornell Univ., Dept. of Astron. 402 Space Sci. Building Ithaca, NY 14853-6801, USA.

Summary: We analyzed polarimetric data for the Martian disk obtained by the Hubble Space Telescope (HST) at the 2003 opposition of Mars. We found transient polarimetric features and studied their relation with surface and atmosphere. We found optically thin clouds that are strongly polarizing in ultraviolet light. The clouds likely are related to condensing ice in the atmosphere, since such features can be formed by micron-scale particles of regular shape and similar size.

Introduction: Planetary surfaces and atmospheres affect the polarization state of scattered solar light. The degree of linear polarization P depends on wavelength λ and illumination/observation geometry (phase angle α). Size of scatterers, their composition, shape, and orientation are responsible for polarization degree variations. The Martian surface is composed of scatterers (soil particles) of different sizes and aggregates of small grains. The atmosphere contains molecules and small particles (permanent sub-micron dust haze) of the clean atmosphere, mists and clouds consisting of ice crystals, and comparatively large suspended particles from dust storms. Earlier Earth-based polarimetric observations of Mars in visible light are presented in [1].

HST polarimetric data: The HST observation program #9738 [2] was carried out at the time of closest Earth-Mars encounter as Mars passed within 0.372 AU of Earth. Five series of images of Mars were taken on Aug. 24, just before the closest approach and on Sept. 5, 7, 12, and 15. The phase angles α at the observation moments were 6.4, 8.2, 9.7, 13.6, and 15.9°, respectively. The image scale was about 7 km/pixel at the disk center (the highest spatial resolution ever achieved from Earth). Disk center in all images was located at 19°S 20-35°W showing the distinctive features of Valles Marineris, Terra Meridiana and surroundings. The season on Mars was summer in the southern hemisphere (the areocentric longitude of the Sun $L_S = 247 - 261^\circ$).

Within this observation program, for the first time, HST observations of Mars included imaging polarimetry. The observations were done with the Advanced Camera for Surveys (ACS) with 3 polarization filters [3]. We used polarization data obtained in combination with two ultraviolet wide-band spectral filters F250W and F330W, and a wide-band blue filter F435W. The number in the filter name is approximately the effective wavelength in nm.

Data processing: The standard dark current, flat field, and geometric distortion calibrations were performed routinely by the HST data retrieval facility.

We then identified and removed the cosmic-ray tracks from the images using an original heuristic algorithm for cosmic rays identification [4]. After spatially coregistering the images obtained with the three polarizers, we derived Stokes parameters of scattered light. To perform the latter step, we derived polarimetric calibration information from calibrating observations of a standard star (HST programs 9586, 9661, 10055) and observations of Mars themselves, making use of symmetry requirements for the center of the disk (see [5] for details).

Transient polarization clouds: Using the normalized Stokes parameters we made images of P for the whole Martian disk for all observation dates. These images reveal transient high-polarization features. These features vary in size, polarization degree, and location. They were best expressed on Sept. 5 and 7, and disappeared after that. The detailed view of polarization degree distribution in the southwestern part of the planetary disk on Sept. 7 is presented in Fig. 1. The most prominent polarization features (red-color-coded) have polarization as high as 3%, the polarization plain is oriented close to the scattering plane. Visual inspection confirms that these features coincide with faint semitransparent clouds.

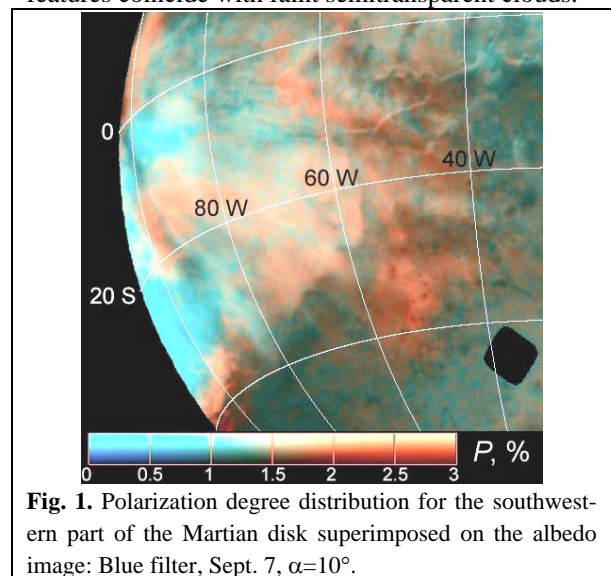


Fig. 1. Polarization degree distribution for the southwestern part of the Martian disk superimposed on the albedo image: Blue filter, Sept. 7, $\alpha=10^\circ$.

The surface albedo features (Thaumasia Planum, Ophir Planum etc.) and Valles Marineris topography remain visible through these faint clouds. The spatial distribution of polarization differs from UV to blue filter, but locations of the major transient polarization maxima are the same in both the filters. We emphasize that the densest clouds (most optically thick) show the lowest polarization in the filters. Only the transition zones characterized by the presence of

faint semi-transparent clouds show the polarization excess. To illustrate this conclusion we compared albedo and polarization profiles over the most interesting region characterized by dramatic changes in polarization degree and cloud density. Fig. 2 shows an image in the UV-330-nm filter for the same part of the disk as in Fig. 1. A complicated clouds system (light shades) with gradual brightness changes and rather dark surface details visible through clear atmosphere are seen.

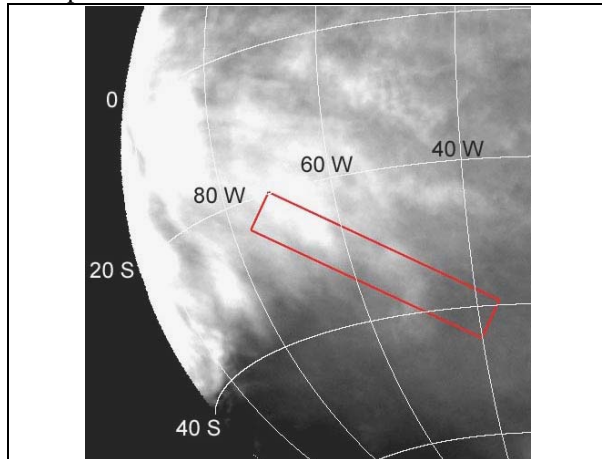


Fig. 2. Albedo image of the southwestern part of the Martian disk in the UV filter F330W, $\alpha=10^\circ$. Red outlined region is discussed in text.

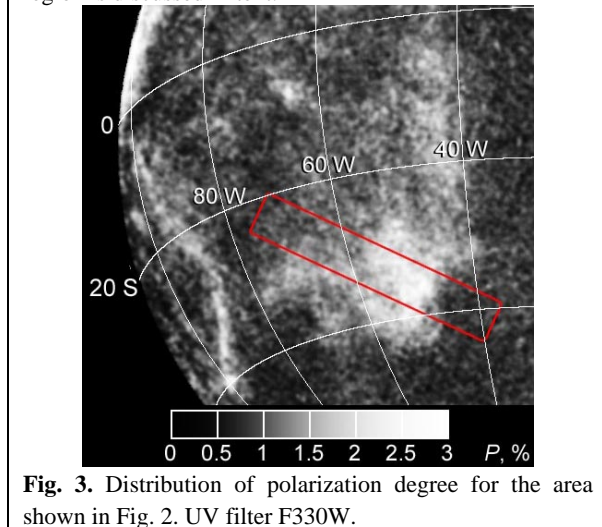


Fig. 3. Distribution of polarization degree for the area shown in Fig. 2. UV filter F330W.

The distribution of P for the same filter is presented in Fig. 3. To suppress inevitable noise and accentuate major polarization changes we slightly smooth the P distribution with a Gaussian filter. The red-outlined rectangle in Figs. 2, 3 cover the area from the northern part of the Argyre Basin to the highest Thaumasia Planum and include the major portion of albedo and polarization dynamic range in the images. Fig. 4 shows the albedo-polarization correlation diagram for the outlined region. It is seen that both the transparent atmosphere (dark areas) and bright clouds show typically low polarization values, while the faint clouds have abnormally high polarization degree. Note, however, that in other portions

of the disk, there are intermediate-brightness semi-transparent clouds without polarization anomalies.

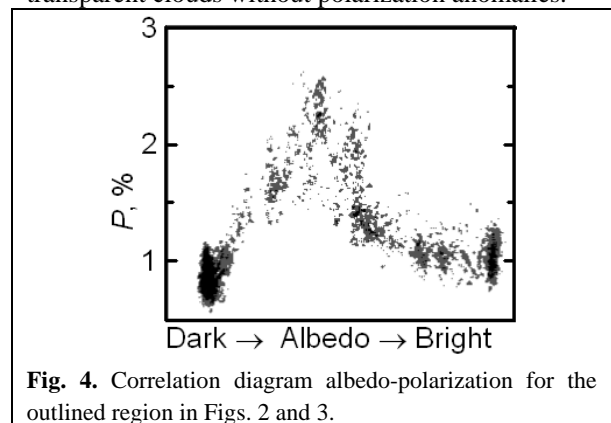


Fig. 4. Correlation diagram albedo-polarization for the outlined region in Figs. 2 and 3.

Atmospheric properties from TES: We retrieved Mars Global Surveyor Thermal Emission Spectrometer (TES) atmospheric dust opacity ($9.7 \mu\text{m}$) and ice opacity ($12.1 \mu\text{m}$) data for the dates. Unfortunately, no MGS tracks crossed the areas of high polarization. The data show that the atmosphere is rather dusty (which is typical for this season), but no particular large-scale dust-lifting events occur in the imaged part of Mars. TES data show a slightly higher ice opacity in the entire western portion of the disk where the polarimetric clouds are observed.

Discussion: Low polarization of bright non-transparent clouds is caused by well developed multiple scattering between aerosol particles in these clouds. This, in fact, explains their high brightness. Multiple scattering in the optically thin clouds is insignificant, and polarization produced by single scattering is preserved. Scattering in a clear atmosphere is dominated by molecular scattering, which follows the Rayleigh scattering law. Therefore, the polarization is normal to the scattering plane and quadratically approaches zero when the phase angle tends toward zero. Thus, a clear atmosphere produces low P in our case.

High polarization of the optically thin clouds suggests that they are made of scatterers having regular shape and similar size. The drop-off in the absolute polarization that occurs when the observation wavelength increases, suggests an upper particle-size limit in the submicron region. Such aerosols may be the result of the initial stages of nucleation of H_2O ice crystals on submicron dust.

References: [1] Ebisawa, S. and A. Dollfus 1993. *Astron. and Astrophys.* 272, 671-686. [2] Bell, J., et al. 2003. *Eos Trans. AGU*, 84(46), Fall Meet. Suppl., Abstract P12C-01. [3] Pavlovsky, C., et al. 2002. *ACS Instrument Handbook*, Version 3.0, Baltimore: STScI. [4] Shkuratov, Yu., et al. 2004. *LPSC*. 35th. Abstract # 1435. LPI Houston. [5] Yu. Shkuratov, et al., *Icarus*, submitted, 2004.